An Investigation on the Inhibitory Action of Modified Almond Extract on the Corrosion of Q235 Mild Steel in Acid Environment

A. O. James[1], N. B. Iroha[2*]

[1](Department of Pure and Industrial Chemistry, University of Port Harcourt, Nigeria)
[2*](Department of Chemistry, Federal University, Otuoke, Nigeria)
Corresponding author: N. B. Iroha

Abstract : *The effect of modified almond extract (MAE) as inhibitor for the corrosion of Q235 mild steel in 0.5 M H_2SO_4 was investigated using weight loss, electrochemical impedance spectroscopy (EIS) and potentiodynamic polarization (PDP) techniques. Scanning electron microscopy (SEM) analysis was employed as characterization technique. The results from EIS and weight loss techniques showed a good inhibition efficiency which increased with increase in extract concentration. Polarization results indicated MAE to be a mixed inhibitor in 0.5 M H_2SO_4 environment, having effect on both the anodic and cathodic partial reactions. MAE inhibits the corrosion of Q235 mild steel by an adsorption mechanism, which follows Freundlich adsorption isotherm. SEM analyses revealed that the corrosion process was retarded in the presence of inhibitor in the acid environment.*
Keywords: *Adsorption mechanism, characterization technique, corrosion inhibitor, mild steel, Modified almond extract.*

I.   Introduction

The use of corrosion inhibitors is very common among the several methods of corrosion control and prevention. Inhibitors are chemicals that are used directly or indirectly on a metal surface to protect it from its environment. Applications of inhibitors is somewhat varied, frequently playing a crucial role in chemical industries, oil and gas industries, engine coolants, heavy industrial manufacturing, automatic transmission fluids, water treatment facility, cutting fluids, water-containing hydraulic fluids, ferrous metal cleaners, water treatment chemicals, automotive component manufacture etc., to reduce localized corrosion and sudden failure of materials [1]. The increasing ecological consciousness, together with the rigid environmental regulations have necessitated the development of environmentally friendly corrosion inhibitors. These inhibitors are being used to replace most inorganic and synthetic inhibitors which though proven to be effective inhibitors are hazardous to human health or the environment in combating corrosion.

The extracts from dried stems, leaves, fruits, bark, seeds and roots of plants have been reported to be effective and eco-friendly inhibitors of metallic corrosion in acidic media [2-9]. This is because these plant extracts serve as rich sources of phytochemicals like tannins, alkaloids, saponins, flavonoids, glycosides, terpenoids, carbohydrates, fats and oils, among others which are known to contain heteroatom such as O, N, and S and multiple bonds in their molecules through which they are adsorbed on the metal surface [10]. They achieve this by providing good adsorption sites unto the metal surface via the residual lone pair of electrons on the hetero atoms present in the molecular structure of the plants molecules. The rate of adsorption is dependent on the inhibitor structure and concentration, composition of the metal and that of the corrodent as well as temperature.

The almond plants are in abundance in the northern and eastern part of Nigeria. The leaves, bark, and root of this plant are rich in tannins which can be described as any group of naturally occurring phenolic compounds. Tannins are known to possess corrosion inhibitive properties on metals, particularly on mild steel [11]. Their basic structure consists of garlic acid residues which are linked to glucose via glycosidic bonds. Thus tannins have an array of hydroxyl and carboxyl groups through which the molecules can adsorb on corroding metallic surfaces. Furfural, on the other hand, is an aldehyde of furan and is a yellow oily liquid in pure form, but tends to turn brown upon prolonged exposure to air and moisture. Furfural can be derived from a variety of agricultural by products, including corncobs, oat, wheat bran, peanut, among others. In our laboratory, furfural have been used to form a resin with red onion skin [12] and red peanut skin [13], and the resins acted as effective inhibitors for aluminium and mild steel corrosion respectively in acidic environment.

The purpose of the present work is to investigate the inhibitory action of the resin formed from almond leaves extract and furfural from peanut husk on the corrosion of Q235 mild steel in 0.5 M H_2SO_4 solutions using

---

weight loss, electrochemical impedance spectroscopy (EIS) and potentiodynamic polarization (PDP) techniques. The surface of the samples was analyzed using scanning electron microscopy (SEM) to study the effect of the inhibitor on mild steel surface.

II. Experimental

Materials Preparation

Q235 mild steel sheet used for this study has the following weight percentage composition: C, 0.30; Mn, 0.30; P, 0.045; Si, 0.30; Cr, 0.064; S, 0.050; Ti, 0.04; Cu, 0.040 and the balance Fe. Each Q235 mild steel sheet, which was 0.14 cm in thickness, was mechanically pressed-cut into coupons of dimension 2 cm × 3 cm for weight loss experiments, 1 cm × 2 cm for electrochemical measurements, and 2 cm × 2 cm for surface analysis examination. The coupons were prepared and cleaned as described elsewhere [13]. The blank corrodent was 0.5 M H_2SO_4 solution.

The almonds leaves were gotten at the ofrima car park, University of Port Harcourt, Nigeria. The fallen leaves were picked and clean properly to remove any dust and sand particles. It was then washed, dried with an oven and ground to powdered form. Weighed amount of the powder was soaked in water contained in a beaker and left to stand for 48 h. The suspension was shaken vigorously and filtered using filter paper. The filtrate (extract) was dried using a water bath and then stored.

Furfural used in this study was obtained from peanut husk by acid hydrolysis. Weighed amount of the dried and powdered peanut husk, sieved using a 60 mesh screen and 4.5 M HCl solution were used for the acid hydrolysis as described elsewhere [12]. The furfural was used within 12 h to modify the almond leaves extract forming a resin which is soluble in water. The resin was prepared in accordance with the method reported in literature [14]. Weighed amount of the almond leaves extract were mixed with 90 mL of furfural and refluxed for 4 h. The resin produced was filtered off, washed free of acid and stored. In preparing the stock solution of the resin, weighed amounts of the resin were refluxed for 3 h in 500 mL of 0.5 M H_2SO_4. The solution was cooled, filtered and stored. From the stock solution, inhibitor test solutions were prepared in concentrations of 0.5, 1.0, 1.5, 2.0 and 2.5 g/L in 0.5 M H_2SO_4.

Weight loss measurement

The pre-weighed coupons were immersed in beakers containing the test solutions of the prepared inhibitors at 303, 313 and 323K. All tests were made in aerated solutions. To determine weight loss with respect to time, the coupons were retrieved from test solutions at 24 h interval, appropriately cleaned, dried, and reweighed. The weight loss was taken to be the difference between the weights of the coupons at a given time and its initial weight. All tests were run in triplicate and the data showed good reproducibility. From the weight loss data, the surface coverage (θ) as a result of adsorption of inhibitor molecules, and inhibition efficiencies of the molecules (η_{WL}) were determined using Eq.(1) and (2), respectively.

$$\theta = \left(1 - \frac{\Delta W_B}{\Delta W_I} \right) \tag{1}$$

$$\eta_{WL} = \theta \times 100 \tag{2}$$

Where ΔW_B and ΔW_I are the weight loss in the absence and presence of the inhibitor respectively.

Electrochemical Techniques

Electrochemical experiments were performed for Q235 mild steel in 0.5 M H_2SO_4 and two concentrations of the resin; 0.5 and 2.5 g/L. Advanced Electrochemical System workstation (PARC Parstart-2273) was used to carry out the test in a typical three-electrode cell of 500 ml capacity. A platinum foil was used as counter electrode and a saturated calomel electrode (SCE) as reference electrodes while mild steel specimen of dimension 2 cm^2 was used as working electrode. The experiment was carried out under naturally aerated condition. EIS measurements were conducted at 30°C for1800s of immersion time to achieve steady open current potential (OCP). The measurements were conducted over a frequency range of 100 kHz – 10 mHz, with a signal amplitude of 5 mV. Impedance data were analyzed using Zsimpwin 3.0 software. PDP measurements were carried out, using standard procedures, at a scan rate of 0.333 mV/s. The potential range of +250 to – 800 mV versus corrosion potential was employed. Powersuite software was used to analyze the polarization data [15]. Charge transfer resistance (R_{ct}) and corrosion current densities were used to calculate the inhibition efficiencies for EIS (η_{EIS}) and PDP (η_{PDP}) studies using Eq.(3) and (4) respectively [16].

$$\eta_{EIS} = \left(1 - \frac{R_{ctB}}{R_{ctI}}\right)100 \tag{3}$$

$$\eta_{PDP} = \left(\frac{I_{corr}^{b} - I_{corr}^{i}}{I_{corr}^{b}}\right)100 \tag{4}$$

where R_{ctI} and R_{ctB} are measured charge transfer resistances with and without the inhibitor respectively, while I_{corr}^{i} and I_{corr}^{b} are the measured corrosion current densities with and without inhibitor respectively. The magnitude of the double layer capacitance (C_{dl}) of the adsorbed film was evaluated using Eq.(5) [17].

$$C_{dl} = \left(Y_{o} R_{ct}^{n-1}\right)^{1/n} \tag{5}$$

where (Y_o) is the magnitude of constant phase element (CPE), n is a constant obtained from the phase angle given that (j2 = -1) and n = $2\alpha/(\pi)$.

Scanning Electron Microscopy (SEM)
         The mild steel samples were examined for surface analysis before and after immersion in the test solution by XL-30FEG scanning electron microscope. The test coupons were immersed in 0.5 M H_2SO_4 solutions in the absence and presence of 1.5 g/L MAE for 24 h. The coupons were retrieved from the test solution, washed with distilled water, dried and used for SEM analysis.

III.   Results and Discussion
Weight Loss Measurements
         The variation of Q235 mild steel weight loss with inhibitor concentration in the absence and presence of MAE at different temperatures in 0.5 M H_2SO_4 is given in Fig. 1. An increase in corrosion rate with rise in temperature is observed in both uninhibited and inhibited solutions. Fig. 1 clearly reveals that MAE effectively inhibits the corrosion of mild steel in 0.5 M H_2SO_4, which becomes more pronounced with increase in the concentration of MAE. This implies that the inhibition process is dependent on the amount of the inhibiting species present in the system. The change in the inhibition efficiency values with the inhibitor concentration at different temperatures is given in Fig. 2, where it can be seen that the inhibition efficiency increases with increase in the concentration of MAE in 0.5 M H_2SO_4. This increase in the inhibition efficiency values with an increase in MAE concentration is due to an increase in the metal surface area covered by the inhibitor.
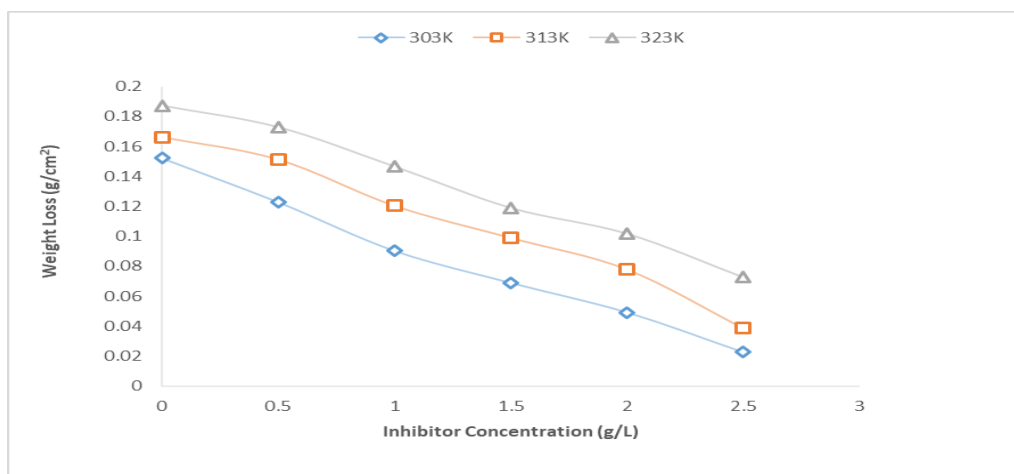
Fig. 1: Variation of mild steel weight loss with Inhibitor concentration in the absence and presence of MAE at different temperatures in 0.5 M H_2SO_4.
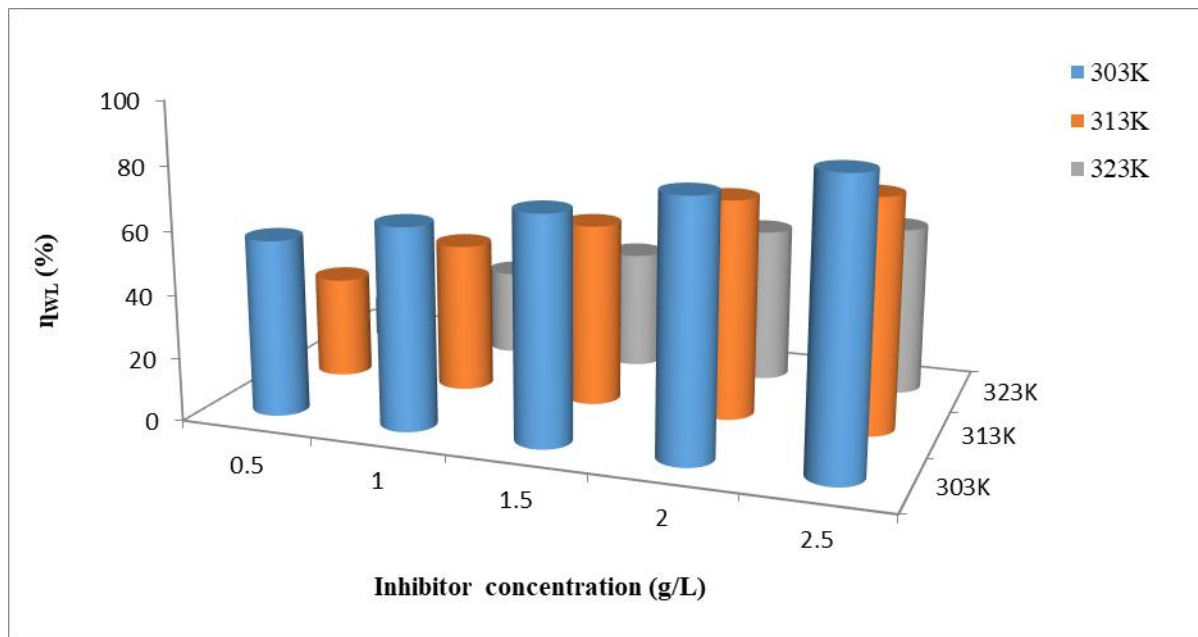
Fig. 2: Variation of Inhibition Efficiency with Inhibitor concentration for Q235 mild steel in 0.5 M H_2SO_4 containing MAE at different temperatures

PDP Measurements

Potentiodynamic polarization (PDP) measurements were therefore carried out to assess the influence of MAE on the kinetics of the anodic and cathodic reactions. Fig. 3 presents the potentiodynamic polarization curves for Q235 mild steel in 0.5 M H_2SO_4 in the absence and presence of selected concentrations of MAE. The mild steel specimen revealed active dissolution and there was no proof of passivation in the studied potential range. Electrochemical corrosion parameters such as corrosion potential (E_{corr}), corrosion current density (I_{corr}), cathodic and anodic Tafel slopes (b_c, b_a) obtained from polarization curves by Tafel extrapolation method and the corresponding inhibition efficiency (η_{PDP}) values at different inhibitor concentrations are given in Table 1.

The data shown therein reveals that when MAE was added the I_{corr} decreased compared to the uninhibited solution and this tendency continued with an increase in the concentration of MAE. The parallel cathodic Tafel lines suggested that the addition of the inhibitor to the 0.5 M H_2SO_4 solution does not modify the hydrogen evolution mechanism or the reduction of H^+ ions at the mild steel surface, which occurs mainly through a charge transfer mechanism [18].

As expected, the addition of the inhibitor impeded the anodic metal dissolution process and also the cathodic H^+ ion reduction [19], indicating that MAE exhibits both cathodic and anodic inhibition effects, but no outstanding effect was noticed on the E_{corr} values. It has been suggested that if the displacement in E_{corr} on addition of inhibitor exceeds 85 mV, the inhibitor could be classified as cathodic or anodic type and if the displacement is lower than 85 mV, then the inhibitor may be regarded as mixed-type [20]. Therefore, from the observation, MAE can be classified as a mixed type inhibitor in 0.5 M H_2SO_4 solution. Also, at over voltages that are higher than circa -350 mV (SCE), it was noticed that metal dissolution was more compared to MAE adsorption.

The I_{corr} values decrease steadily from the blank value with the increase in inhibitor concentration from 0.5 to 2.5 g/L. Since, the corrosion current is proportional to the magnitude of the corrosion reaction. The decrease in I_{corr} clearly confirms that the inhibition efficiency increases with an increasing MAE concentration [21].
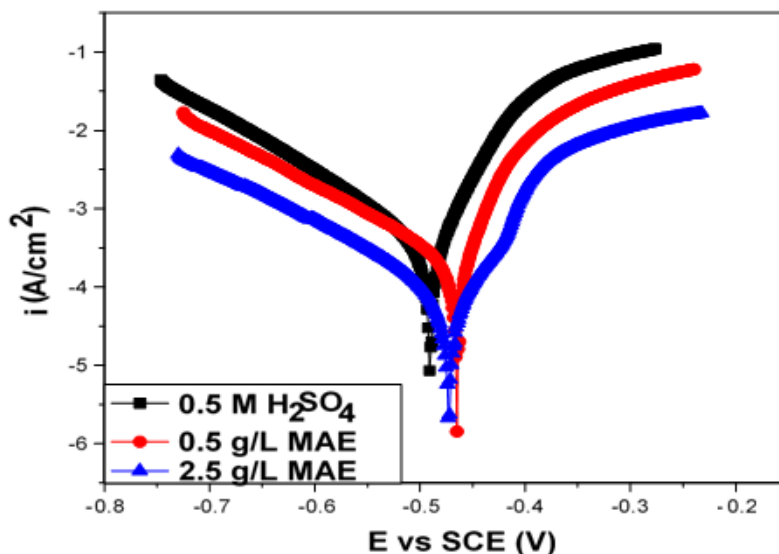
Fig. 3: Potentiodynamic polarization curves of Q235 mild steel in 0.5 M H$_2$SO$_4$ solution without and with MAE

Table 1: Polarization parameters for Q235 mild steel in 0.5 M H$_2$SO$_4$ without and with selected concentrations of MAE

Concentration (g/L)	E_{corr} (mV vs SCE)	I_{corr} (μA cm^{-2})	b_a (mV dec^{-1})	b_c (mV dec^{-1})	η_{PDP} (%)
Blank	-490.4	784.3	107.9	94.8	
0.5	-473.7	176.9	83.5	86.4	77.4
2.5	-454.1	85.1	83.1	83.9	89.1

EIS Measurements

Nyquist plots for Q235 mild steel in 0.5 M H$_2$SO$_4$ solution in the absence and presence of different concentrations of MAE are given in Fig. 4. Obtained impedance diagrams have appearance of one capacitive contribution represented by one semi-circle for all solutions examined. The curves for all the tested solutions are alike shape-wise showing that the dissolution mechanism is same notwithstanding the presence or absence of MAE [22]. However, further inspection of Fig. 4 reveals a larger diameter of the capacitive semicircle in the presence of MAE compared to that of the blank H$_2$SO$_4$; with further enhancement in the diameter of the capacitive loop with increase in MAE concentration. This demonstrates that introduction of MAE into the corrosive medium increased resistivity towards charge transfer at the metal-solution interface and brought about a reduction in the corrosion rate as a result of its inhibitive effect [23]. The areas of high frequency intercept with their real axis in the Nyquist plots are attributed to the solution resistance (R_s) and the areas of low frequency intercept with their real axis are related to the charge transfer resistance (R_{ct}).

The measured values of the various impedance parameters shown in Table 2, were extrapolated by fitting to the relevant circuit models R$_s$ (Q$_{dl}$R$_{ct}$), which have been employed earlier to model the metal/acid interface [24, 25]. The CPE is used here in place of a capacitor to account for the deviations from ideal dielectric behavior resulting from the inhomogeneous nature of the electrode surfaces. Considering the data presented in Table 2, it is clear that MAE increased the R_{ct} values in the presence of the inhibitor compared with the uninhibited solution. The R_{ct} values increase with increasing inhibitor concentration. This is due to increasing surface coverage by inhibitors which leads to an increase in η$_{EIS}$ values with increasing inhibitor concentration. It is also observed from the table that inhibition efficiency increased with a decrease in double layer capacitance (C$_{dl}$) in the presence of MAE compared to the blank. The decrease in the values of C$_{dl}$ might be attributed to the gradual replacement of water molecules by the adsorption of the inhibitor molecules at the steel/electrolyte interface [26] resulting in an increase in the thickness of electrical double layer or/and a decrease in local dielectric constant.
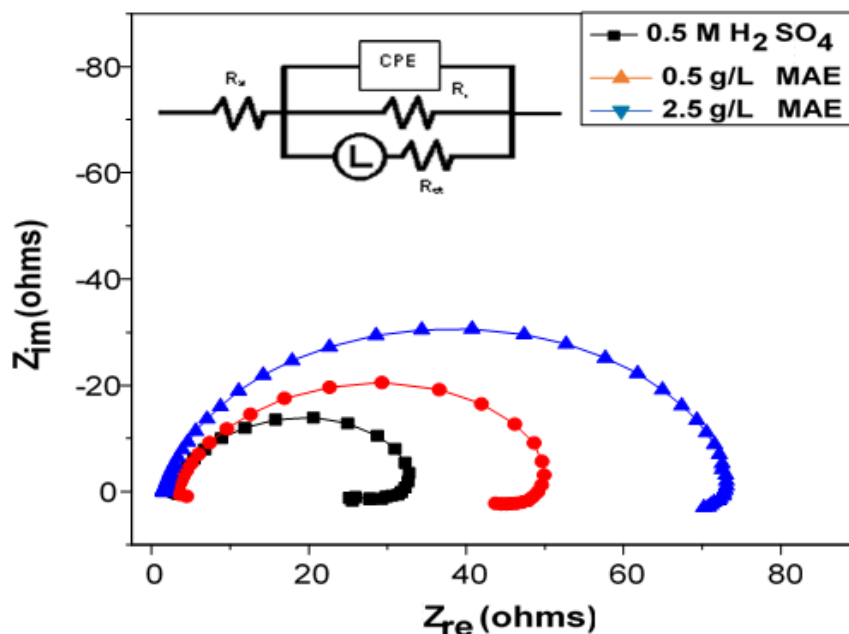
Fig. 4. Nyquist plot of the electrochemical impedance spectra on Q235 mild steel in 0.5 M H_2SO_4 in the presence and absence of MAE.

Table 2: Electrochemical Impedance Parameters of Q235 mild Steel in 0.5 M H_2SO_4 in the Absence and Presence of MAE

Concentration (g/L)	R_s (Ω cm^2)	R_{ct} (Ω cm^2)	n	Y_o (μ Ω^{-1}s^{2}cm^{-2})	C_{dl} (μFcm^{-2})	η_{EIS} (%)
Blank	2.07	29.2	0.89	215.8	102.7	-
0.5	3.01	83.6	0.88	119.2	83.4	65.1
2.5	3.24	121.5	0.89	93.6	54.8	76.0

Adsorption Isotherm

The adsorption of organic inhibitors on a corroding metal surface is essential step in the inhibition mechanism and is often described by two main types of interaction; chemical adsorption and physical adsorption. The adsorption of the inhibitor is influenced by the nature and the charge of the metal, the chemical nature of the inhibitor, distribution of the charge in the molecule, and the type of electrolyte [27]. Adsorption behaviour is usually described and analyzed with adsorption isotherm model like Freundlich, Flory-Huggins, Temkin, Bockris-swinkles, Langmuir and Frumkin adsorption isotherms. To gain insight into the mode of adsorption of the extract on mild steel surface, the surface coverage values from gravimetric technique were theoretically fitted into different adsorption isotherms and the values of correlation coefficient (R^2) were used to determine the isotherm that fits best. Freundlich adsorption isotherm was found to fit the experimental data well. Freundlich isotherm is given by the expression:

$$\ln \theta = \ln K_{ads} + n \ln C \tag{6}$$

where θ is the degree of surface coverage, K_{ads} is the adsorption equilibrium constant, n is the interaction parameter and C is the inhibitor concentration. Fig. 5 shows the plot of $\ln \theta$ against $\ln C$. Linear plots were obtained for MAE in both 0.5 M H_2SO_4 with good correlation coefficient (R^2) which suggests that adsorption of the inhibitor follow Freundlich adsorption isotherm. The adsorption equilibrium constant, K_{ads} decreases with increase in temperature (Table 1), such data explains the decrease in the inhibition efficiency with increasing temperature. The free energy of adsorption (ΔG), which is the most important thermodynamic adsorption parameter, is related to the adsorption constant (K_{ads}) by Eq.7:

$$\Delta G = -RT \ln(55.5 K_{ads}) \tag{7}$$

where 55.5 is the water concentration in solution, R is the ideal gas constant, and T is the absolute temperature. Table 1 shows the values calculated from the Freundlich isotherm. The negative values of ΔG indicate the spontaneity of the adsorption process and the stability of the adsorbed layer on the mild steel surface. The values of ΔG_{ads} obtained indicate that adsorption of MAE on mild steel in 0.5 M H_2SO_4 occurs via

physical adsorption mechanism. Generally, values of ΔG less negative than -40 kJ/mol signify physical adsorption.
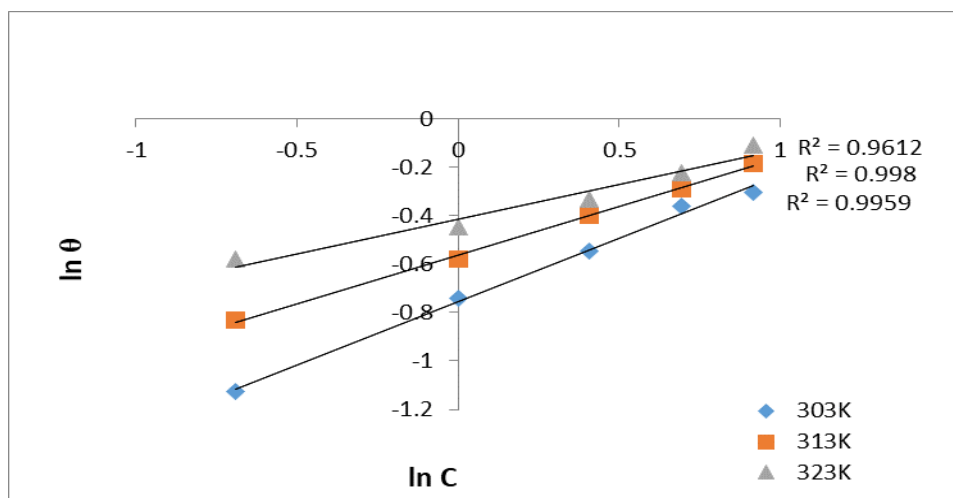

Fig. 8. Freundlich adsorption isotherm for MAE on Q235 mild steel in 0.5 M H$_2$SO$_4$ solution at different temperatures

Table 1. Calculated Adsorption parameters from Freundlich adsorption isotherm for Q235 mild steel corrosion in 0.5 M H$_2$SO$_4$ at different temperatures

Temp. (K)	K_{ads} x 10^5	ΔG_{ads}(kJ/mol)	R^2
303	2.62	-19.42	0.961
313	2.54	-17.84	0.998
323	2.49	-16.29	0.995

Effect of Temperature

The effect of temperature on the corrosion rate of Q235 mild steel in 0.5 M H$_2$SO$_4$ containing different concentrations of MAE was tested by weight loss measurements over a temperature range from 303 to 323K. The result presented in Fig. 1 shows that corrosion rates in both uninhibited and inhibited acids increased with rise in temperature. Also, MAE is seen to maintain its inhibiting effect at all temperatures. The result in Fig. 2 reveals a decrease in inhibition efficiency with increasing temperature for mild steel in 0.5 M H$_2$SO$_4$. Decrease in inhibition efficiency with increase in temperature is suggestive of physical adsorption of MAE onto the mild steel surface.

To calculate activation energy (E_a) and other activation thermodynamic parameters of the corrosion reaction such as the enthalpy of activation (ΔH^*) and the entropy of activation (ΔS^*), the Arrhenius equation (8) and the Eyring's transition state equation (9) were employed:

$$\ln k = \ln A - \frac{E_a}{RT} \tag{8}$$

$$k = \left(\frac{RT}{Nh}\right)\exp\left(\frac{\Delta S^*}{R}\right)\exp\left(\frac{\Delta H^*}{R}\right) \tag{9}$$

where k is the corrosion rate, A is the pre-exponential factor, R the universal gas constant, T is the absolute temperature, h is the Planck's constant and N is the Avogadro's number.

The activation energy is calculated from the slope of the plots of $\ln k$ versus $1/T$ (Fig. 9). Plots of Log (k/T) as a function of $1/T$ (Fig. 10) give a straight line with a slope of ($-\Delta H^*/2.303R$) and an intercept of (log $R/Nh + \Delta S^*/2.303R$) from which the values of ΔH^* and ΔS^* were calculated. The calculated values of the activation thermodynamic parameters are listed in Table 2. It could be seen from Table 2 that the presence of MAE increases the values of E_a as compared to the blank acid solutions, indicating physical adsorption of the extracts on the metal surface [13, 28]. The positive values of ΔH^* both in absence and presence of inhibitor reflect the endothermic nature of the mild steel dissolution process in the 0.5 M H$_2$SO$_4$. The activation enthalpies are also seen to vary in the same manner as the activation energies, supporting the proposed inhibition mechanism. The values of ΔS^* in the presence and absence of MAE are large and negative implying that the activation complex is the rate determining step and represents association rather than dissociation. This clearly indicates that a decrease in disorder takes place on going from reactants to the activated complex [29]
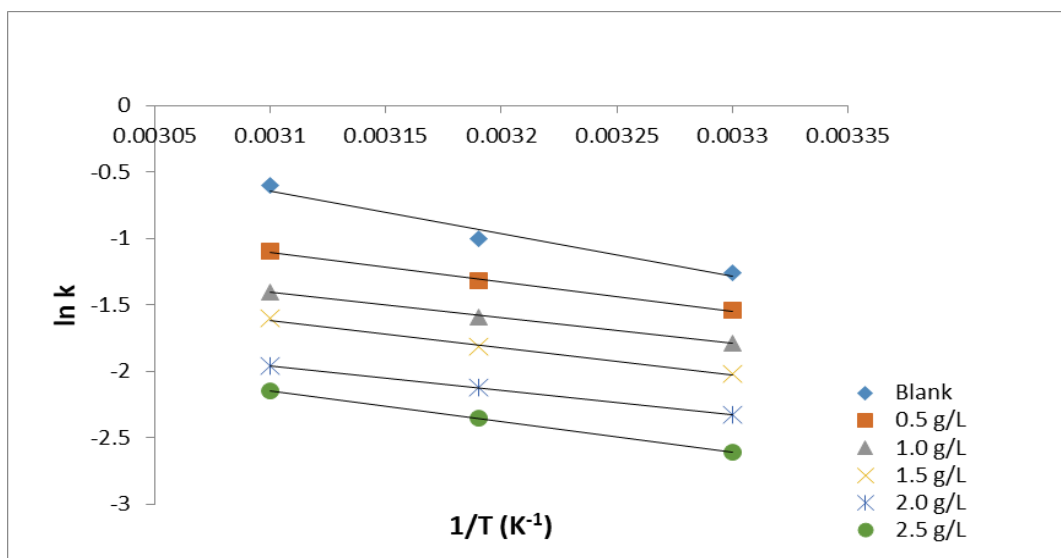
Fig. 9: Arrhenius plots for Q235 mild steel corrosion in 0.5 M H_2SO_4 without and with different concentrations of MAE
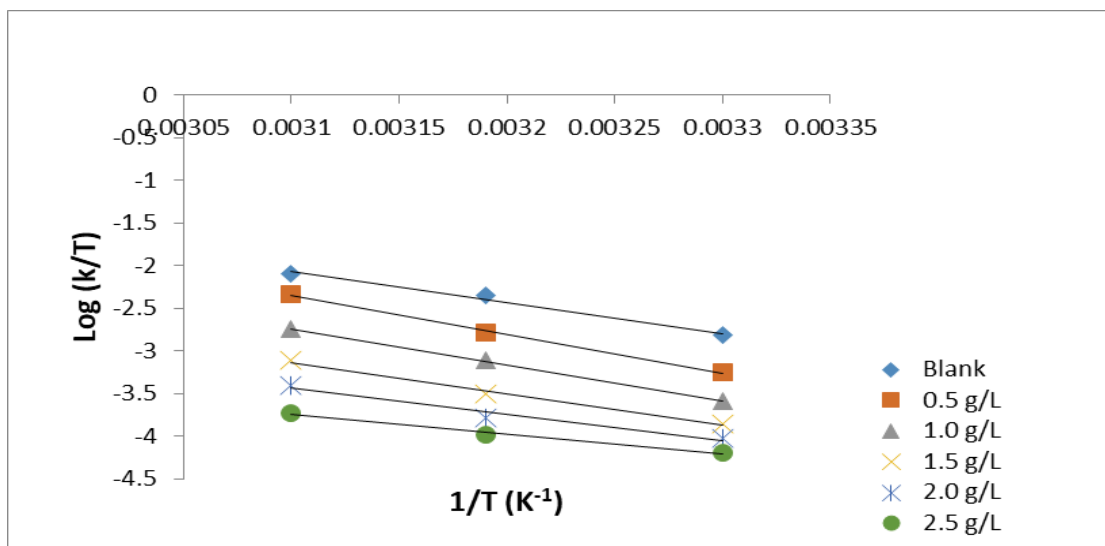

Fig. 10: Eyring plots for Q235 mild steel corrosion in 0.5 M H_2SO_4 without and with different concentrations of MAE

Table 2. Calculated values of activation parameters for Q235 mild steel corrosion in 0.5 M H_2SO_4 in the absence and presence of MAE

Concentration (g/L)	E_a (kJ/mol)	ΔH^* (kJ/mol)	ΔS^* (J/mol/K)
Blank	39.75	26.35	-185.42
0.5	42.00	28.21	-181.22
1.0	43.93	30.00	-175.24
1.5	46.21	32.94	-162.10
2.0	48.09	34.71	-159.02
2.5	55.24	39.24	-126.33

SEM observations

The SEM images were recorded to establish the interaction of inhibitor molecules with the metal surface. Fig. 11a–b shows the scanning electron micrographs for mild steel after immersion for 24 h in 0.5 M H_2SO_4 solution without and with optimum concentration of MAE. Results show that the surface of the metal sample in 0.5 M H_2SO_4 solution without inhibitor (Fig.11a) was severely damaged by acid attack. Examination of Fig. 11b reveals that the specimens immersed in the inhibitor solutions are in better conditions having smooth surfaces compared with that of the surface immersed in 0.5 M H_2SO_4 alone. This indicates that MAE molecules

hinders the dissolution of mild steel by forming a protective film on the metal surface and thereby reduces the corrosion rate.

(a)   (b)
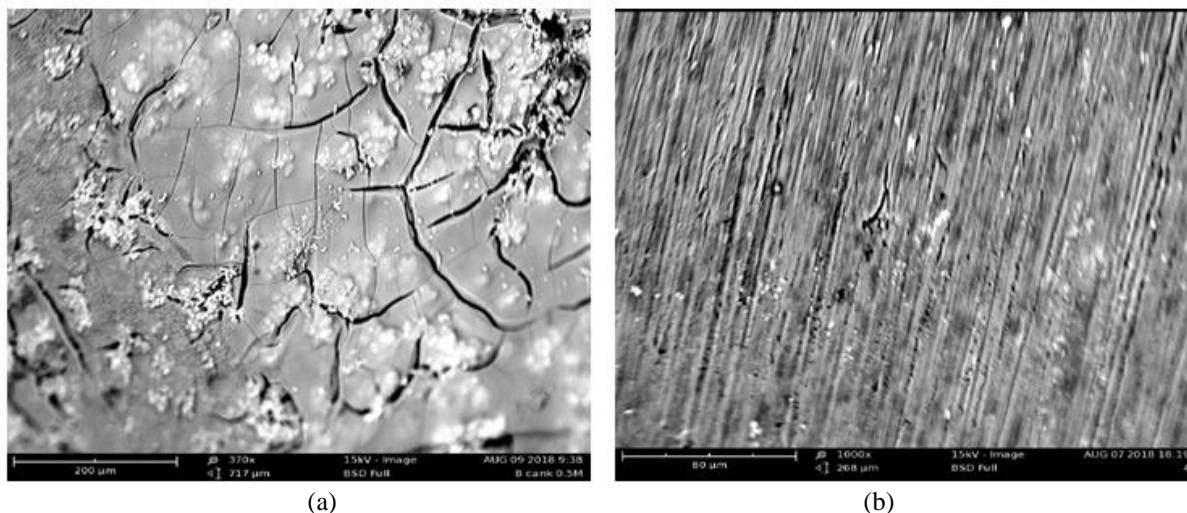
Fig. 11. SEM micrographs of Q235 mild steel surfaces in (a) uninhibited and (b) MAE inhibited 0.5 M H_2SO_4 solution

IV.   Conclusion

MAE was found to function as an inhibitor of mild steel corrosion in 0.5 M H_2SO_4 solution. The adsorption of the inhibitor on the mild steel surface is spontaneous and supports the mechanism of physical adsorption. Polarization studies indicate the inhibitor to be of a mixed type, inhibiting both cathodic as well as anodic reactions. The rate of corrosion of the mild steel in 0.5 M H_2SO_4 is a function of the concentration of the inhibitor. This rate decreased as the concentration of the inhibitor is increased. The percentage inhibition efficiency of this inhibitor decreased as the temperature increases which indicate that physical adsorption was the predominant inhibition mechanism. The corrosion process was inhibited by adsorption of the inhibitor molecule on the mild steel surface which is visible with SEM.

References

[1]. T. R. Loto, C. A. Loto, I. P. A. Popoola and M. Ranyaos, Pyrimidine Derivatives as Environmentally-Friendly Corrosion Inhibitors, *International Journal of the Physical Sciences, 6(15),* 2012, 3616-3623.

[2]. R. Saratha and V. G. Vasudha, Emblica Officinalis (Indian Gooseberry) leaves extract as corrosion inhibitor for mild steel in 1N HCL medium, *E-Journal of Chemistry, 7(3),* 2010, 677–684.

[3]. N. B. Iroha and M. A. Chidiebere, Evaluation of the Inhibitive Effect of Annona Muricata. L Leaves Extract on Low-Carbon Steel Corrosion in Acidic Media, *International Journal of Materials and Chemistry, 7(3),* 2017, 47-54.

[4]. N. Kumpawat, A. Chaturvedi and R. K. Upadhyay, A Comparative Study of Corrosion Inhibition Efficiency of Stem and Leaves Extract of Ocimum sanctum (Holy Basil) for Mild Steel in HCl Solution, *Protection of Metals and Physical Chemistry of Surfaces, 46(2),* 2010, 267-270.

[5]. N. B. Iroha and N. A. Madueke, Effect of Triumfetta rhomboidea Leaves Extract on the Corrosion Resistance of Carbon Steel in Acidic Environment, *Chemical Science International Journal, 25(2),* 2018, 1-9.

[6]. A. Singh, I. Ahamad, V. K. Singh and M. A. Quraishi, Inhibition effect of environmentally benign Karanj (Pongamia pinnata) seed extract on corrosion of mild steel in hydrochloric acid solution, *Journal of Solid State Electrochemistry, 15,* 2011, 1087–1097.

[7]. N. El Hamdani, R. Fdil, M. Tourabi, C. Jama and F. Bentiss, Alkaloids extract of Retama monosperma (L.) Boiss. seeds used as novel eco-friendly inhibitor for carbon steel corrosion in 1M HCl solution: electrochemical and surface studies, *Applied Surface Science, 357,* 2015, 1294–1305.

[8]. N. A. Madueke and N. B. Iroha, Protecting aluminium alloy of type AA8011 from acid corrosion using extract from Allamanda cathartica leaves, *International Journal of Innovative Research in Science, Engineering and Technology, 7(10),* 2018, 10251-10258

[9]. N. B. Iroha and A. Hamilton-Amachree, Adsorption and anticorrosion performance of Ocimum Canum extract on mild steel in sulphuric acid pickling environment, *American Journal of Materials Science, 8(2),* 2018, 39-44

[10]. A. Ehsani, M. G. Mahjani, M. Hosseini, R. Safari, R. Moshrefi and S. H. Mohammad, Evaluation of Thymus vulgaris plant extract as an eco-friendly corrosion inhibitor for stainless steel 304 in acidic solution by means of electrochemical impedance spectroscopy, electrochemical noise analysis and density functional theory, *J. Colloid Interface Sci., 490,* 2017, 444–451.

[11]. C. A. Loto, T. R. Loto and I. P. A. Popoola, Corrosion and Plant Extracts Inhibition of Mild Steel in HCl, *International Journal of the Physical Sciences, 6(15),* 2011, 3616-3623.

[12]. N. B. Iroha, O. Akaranta and A. O. James, Red onion skin extract-furfural resin as corrosion inhibitor for aluminium in acid medium, *Der Chemica Sinica, 3(4),* 2012, 995-1001.

[13]. N. B. Iroha, O. Akaranta and A. O. James, Corrosion Inhibition of Mild Steel in Acid Media by Red Peanut skin extract-furfural Resin, *Advances in Applied Science Research, 3(6),* 2012, 3593-3598.

[14]. N. B. Iroha and A. O. James, Assessment of performance of velvet tamarind-furfural resin as corrosion inhibitor for mild steel in acidic solution, *J. Chem Soc. Nigeria, 43(3),* 2018, 510–517.

[15]. M. A. Chidiebere, N. Simeon, D. Njoku, N. B. Iroha, E. E. Oguzie and Y. Li, Experimental study on the inhibitive effect of phytic acid as a corrosion inhibitor for Q235 mild steel in 1 M HCl environment, *World News of Natural Sciences, 15*, 2017, 1-19.

[16]. E. B. Ituen, M. M. Solomon, S. A. Umoren and O. Akaranta, Corrosion inhibition by amitriptyline and amitriptyline based formulations for steels in simulated pickling and acidizing media, *Journal of Petroleum Science and Engineering, 174,* 2019, 984–996.

[17]. N. El Hamdani, R. Fdil, M. Tourabi, C. Jama and F. Bentiss, Alkaloids extract of Retama monosperma (L.) Boiss. seeds used as novel eco-friendly inhibitor for carbon steel corrosion in 1M HCl solution: electrochemical and surface studies, *Appl. Surf. Sci. 357,*2015, 1294–1305.

[18]. S. Kertit, B. Hammouti, Corrosion inhibition of iron in 1M HCl by 1-phenyl-5-mercapto-1,2,3,4-tetrazole, *Appl. Surf. Sci. 93(1),* 1996, 59–66.

[19]. H. K. Sappani and K. Sambantham, Torsemide and Furosemide as Green Inhibitors for the Corrosion of Mild Steel in Hydrochloric Acid Medium, *Industrial and Engineering Chemistry Research 52 (22),* 2013, 7457-7469

[20]. X. Wang, H. Yang and F. Wang, An investigation of benzimidazole derivative as corrosion inhibitor for mild steel in different concentration HCl solutions, *Corrosion Science 53 (1)*, 2011, 113-121

[21]. C. N. Cao, 2004. Corrosion Electrochemistry Mechanism, *Chemical Industrial Engineering Press, Beijing, 235,* 2004.

[22]. M. M. Solomon, H. Gerengi and S. A. Umoren, Carboxymethyl cellulose/silver nanoparticles composite: synthesis, characterization and application as a benign corrosion inhibitor for St37 steel in 15% H_2SO_4 medium. *ACS Appl. Mater. Interfaces, 9,* 2017, 6376–6389.

[23]. E. A. Essien, D. Kavaz, E. B. Ituen and S. A. Umoren, Synthesis, characterization and anticorrosion property of olive leaves extract-titanium nanoparticles composite, *Journal of Adhesion Science and Technology, DOI: 10.1080/01694243.2018.1445800*, 2018, 1-22

[24]. I. B. Obot and N. O. Obi-Egbedi, Adsorption Properties and Inhibition of Mild Steel Corrosion in Sulphuric Acid Solution by Ketoconazole: Experimental and Theoretical Investigation, *Corrosion Science, 52*, 2010, 198-204.

[25]. Z. Tao, S. Zhang, W. Li and B. Hou, Adsorption and Inhibitory Mechanism of 1H-1,2,4-Triazol-l-yl-methyl-2-(4-chlorophenoxy) Acetate on Corrosion of Mild Steel in Acidic Solution, *Industrial and Engineering Chemistry Research 50 (10)*, 2011, 6082-6088

[26]. M. Lagrene′e, B. Mernari, M. Bouanis, M. Traisnel and F. Bentiss, Study of the mechanism and inhibiting efficiency of 3,5-bis(4-methylthiophenyl)-4H-1,2,4-triazole on mild steel corrosion in acidic media. *Corros Sci. 44, 2002*, 573–588.

[27]. E. E. Oguzie, Corrosion inhibition of aluminium in acidic and alkaline media by Sansevieria trifasciata extract, *Corrosion Science*, *9(3),* 2007, 1527-1536.

[28]. S. A. Umoren, I. B. Obot and N. O. Obi-Egbedi, Corrosion inhibition and adsorption behaviour for aluminuim by extract of Aningeria robusta in HCl solution: Synergistic effect of iodide ions, *J. Mater. Environ. Sci. 2(1),* 2011, 60-71.

[29]. M. Abdallah, E.A. Helal and A.S. Founda, Aminopyrimidine derivatives as inhibitors for corrosion of 1018 carbon steel in nitric acid solution, *Corros. Sci. 48 (7)*, 2006, 1639-1654